LAWRENCE
LIVERMORE
NATIONAL
LABORATORY

LLNL-CONF-405994

Diamond-machined ZnSe immersion grating for NIR high-resolution spectroscopy

Y. Ikeda, N. Kobayashi, P. J. Kuzmenko, S. L. Little, C. Yasui, S. Kondo, A. Minami, K. Motohara

August 4, 2008

SPIE Advanced Optical and Mechanical Technologies in Telescopes and Instrumentation
Marseille, France
June 23, 2008 through June 28, 2008

Disclaimer

Diamond-machined ZnSe immersion grating for NIR high-resolution spectroscopy

Yuji Ikeda[a], Naoto Kobayashi[b], Paul J. Kuzmenko[c], Steve L. Little[c], Chikako Yasui[b], Sohei Kondo[b], Atsushi Minami[b], and Kentaro Motohara[b]

[a]Photocoding, 3-16-8-101 Higashi-Hashimoto, Sagamihara, Kanagawa 229-1104, Japan;
[b]Institute of Astronomy, University of Tokyo, 2-21-1 Osawa, Mitaka, Tokyo 181-0015, Japan;
[c]Lawrence Livermore National Laboratory, 7000 East Avenue, Livermore, CA 94550, USA;

ABSTRACT

ZnSe immersion gratings ($n \sim 2.45$) provide the possibility of high-resolution spectroscopy for the near-infrared (NIR) region. Since ZnSe has a lower internal attenuation than other NIR materials, it is most suitable for immersion grating, particularly in short NIR region ($0.8 - 1.4$ μm). We are developing an extremely high-resolution spectrograph with $\lambda/\Delta\lambda = 100,000$, WINERED, customized for the short NIR region, using ZnSe (or ZnS) immersion grating.[1] However, it had been very difficult to make fine grooves on ZnSe substrate with a small pitch of less than 50 μm because ZnSe is a soft/brittle material. We have overcome this problem and successfully machined sharp grooves with fine pitch on ZnSe substrates by nano precision fly-cutting technique at LLNL. The optical testing of the sample grating with HeNe laser shows an excellent performance: the relative efficiency more than 87.4 % at 0.633 μm for a classical grating configuration. The diffraction efficiency when used as an immersion grating is estimated to be more than 65 % at 1μm. Following this progress, we are about to start machining a grating on a large ZnSe prism with an entrance aperture of 23mm $\times$ 50mm and the blaze angle of 70°.

Keywords: Infrared, Spectroscopy, High resolution, Optical device, Immersion grating

1. INTRODUCTION

Immersion grating is a powerful optical device for astronomical spectroscopy which is immersed into an optical material with the high refractive index of n. The maximum spectral resolution (R) of a spectrometer using the immersion grating is well known as,

$$R = \frac{\lambda}{\Delta\lambda} = \frac{2n\phi \tan\theta_{\rm B}}{Ds}, \quad (1)$$

where ϕ is the collimated beam diameter which is deeply related to the overall instrumental volume, $\theta_{\rm B}$ is the blaze angle, D is the telescope diameter, and s is the silt width (e.g., see Yasui et al.[2]). From Eq.(1), immersion grating can provide n times spectral resolution or can reduce the collimated beam, namely instrumental volume, into the size of $1/n$, compared to classical reflective grating (see Fig. 1). Thus, this grating received a lot of attention as a key device for high resolution spectrometer with $R \geq 70,000$ attached to Extremely Large Telescope such as Thirty Meter Telescope[3–5] because very large and heavy cryogenic instruments can be avoided.

We have been developing a high resolution spectrograph, WINERED[1,2,6] (see Fig. 2), which has the possibility of providing high resolution spectra with $R = 100,000$ at the short NIR wavelengths ($\lambda = 0.9 - 1.35$ μm; z, Y, and J bands) using a ZnSe or ZnS immersion grating. Tab. 1 shows requirements of the immersion grating for WINERED. You can see that the size of clear aperture is much smaller than that of spectrometers using a classical reflective echelle grating (for example, the collimated beam of CRIRES/VLT,[7] which is a NIR high-resolution spectrograph with $\lambda/\lambda = 100,000$, has a diameter of 200 mm). However, the immersion grating technology for the NIR wavelengths has not been established yet, except for silicon immersion grating fabricated by the photolithographic technique (e.g., Marsh et al.[8]). In particular, there are several issues for realizing ZnSe

Further author information: (Send correspondence to Y.I.)
Y.I.: E-mail: ikeda@photocoding.com, Telephone: +81 42 774 7960
N.K.: E-mail: naoto@ioa.s.u-tokyo.ac.jp, Telephone: +81 422 34 5032

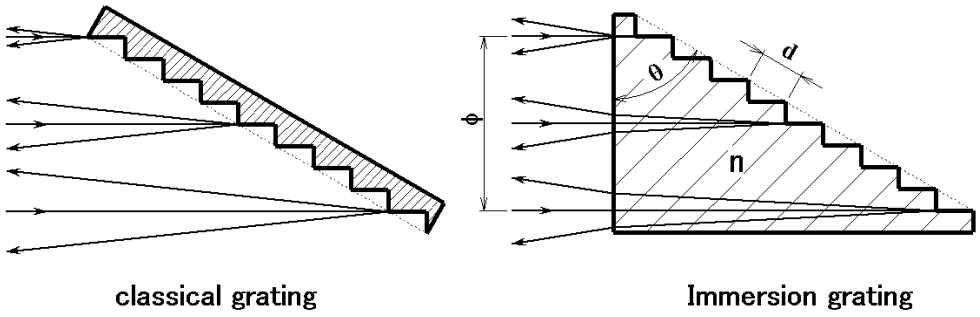

Figure 1. A classical reflective grating and an immersion grating

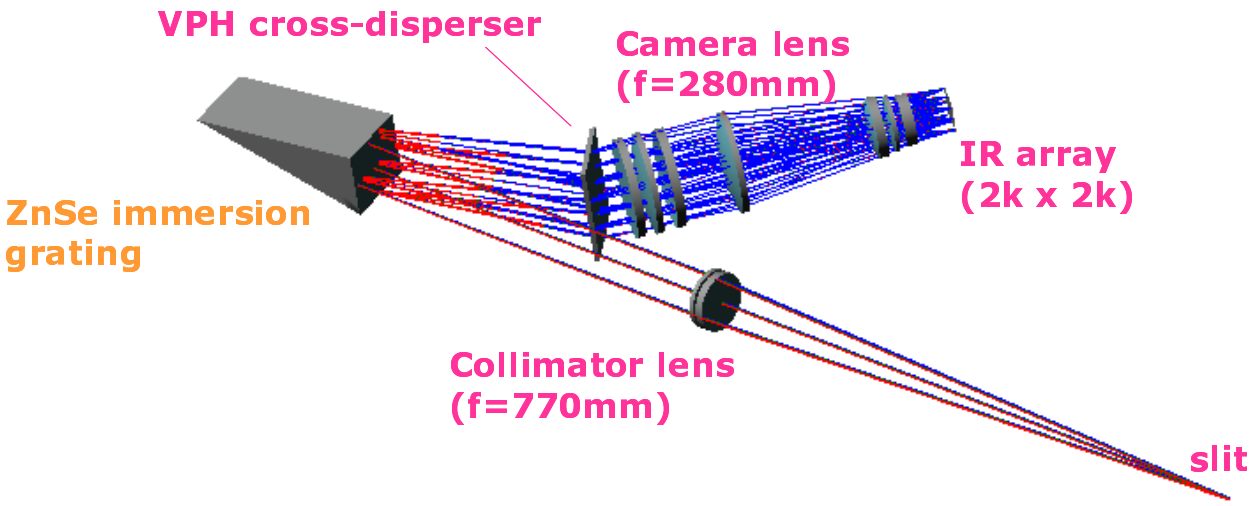

Figure 2. Optical layout of the short NIR high-resolution spectrograph, WINERED. This is the current configuration, which employs the transmissive lens as a collimator but the reflective parabola mirror in the previous version. See Yasui et al.[1] for more details.

or ZnS immersion grating. At first, because the large single crystalline ZnSe and ZnS are difficult to grow and very expensive at present, only poly-crystalline ones by Chemical Vapor Deposition (CVD) are available for immersion grating. Because the CVD-ZnSe and CVD-ZnS are brittle and soft materials, it is difficult to produce the fine grooves on the substrates without any chipping on the groove edge. Second, CVD-ZnSe and CVD-ZnS shows a little attenuation in the short NIR, which could degrade the total throughput of the spectrometer.[9] Therefore, we investigated the possibility using of CVD-ZnSe and CVD-ZnS as an immersion grating material in the short NIR. In Section 2, we describe the internal attenuation of CVD-ZnSe and CVD-ZnS and discuss the maximum efficiency of immersion gratings. In Section 3 and Section 4, we report the fabrication of a sample ZnSe grating using the nano-precision fly-cutting technique, and the optical performance obtained by the optical testings using visible laser. Finally, we introduce the plan of fabrication of a large prism grating and current status in the last section.

2. INTERNAL ATTENUATION OF CVD-ZNSE

Ikeda et al.[9] mention that CVD-ZnS and CVD-ZnSe could show serious internal attenuation at wavelengths less than $\lambda = 1.0$ μm for immersion grating applications. They conclude that the attenuation is mainly attributed to the bulk scattering because of their poly-crystalline nature of the material. Fig.3 is the transmittance considering

material	CVD-ZnSe ($n = 2.45$)	CVD-ZnS multi-spectral grade ($n = 2.3$)
wavelength	$0.9 - 1.4$ μm	$0.9 - 1.4$ μm
groove pitch	31.5 μm	29.6 μm
blaze angle	70 degree	70 degree
diameter of collimated beam	70 mm ϕ	70 mm ϕ

Table 1. Specifications of the immersion grating for WINERED

the internal attenuation for a single block immersion grating with the collimator beam diameter of 70 mm, which is required by WINERED. Unfortunately, an non-negligible part of the incident energy into the immersion grating is lost by the internal attenuation, and in particularly, the transmittance is only about $60 - 70$ % in the shorter wavelengths than $\lambda = 1$ μm.

Alternatively, we propose a mosaic-type immersion grating as shown in Fig. 4. The total optical path in this type grating becomes shorter than a single immersion grating, resulting in the significant recovery of the transmittance *. If adopting a three-stage mosaic-type immersion grating using CVD-ZnSe, the transmittance is estimated to be recovered by 92 % at $\lambda = 1.4$ μm and 87 % at $\lambda = 1.0$ μm. However, we have to take care of the ghost light from the base surface of each small prism grating and the vignetting near the boundary between small gratings if using the mosaic-type immersion gratings.

3. FABRICATION OF ZNSE SAMPLE GRATING

We prepared a CVD-ZnSe flat substrate with a diameter of 25 mm and a thickness of 6.25 mm for fabrication of a test grating. This substrate was polished on one side and rough ground on the other side. We produced grooves with a pitch of 30 μm and a blaze angle of 65° on the half area of the ZnSe substrate (see Fig. 5), by a nano precision fly-cutting technique using the Precision Engineering Research Lathe (PERL II) at Lawrence Livermore National Laboratory (LLNL).[10–12] We obtained the fine grooves with little chipping under the conditions of the spindle speed of 1000 rpm and the feed rate less than 0.4 inch per minute. The details about PERL II and the fabrication of the sample grating are written in the related paper by Kuzmenko et al.[13]

The average surface roughness measured with a Vecco optical profirometer is 4.8 nm (rms). As discussed in the following section, this value is very comfortable as an astronomical immersion grating for the short NIR region. The blaze angle is also estimated to be $61.7° \pm 0.1°$ with the same method to that described by Kuzmenko et al.[13] and Ikeda et al.[14] This discrepancy from the designed value of 65° would be due to an error in shaping of the diamond tools.

4. OPTICAL TESTING AND PERFORMANCE

To examine the optical performance, we exposed a HeNe laser beam with a diameter of 0.6 mm to the sample grating from the air under the Littrow condition. The diffracted light was separated by a beam-splitter, which was aligned with a slight rotation to avoid the stray light reflected from the entrance/exit surfaces, and partly focused on the cooled CCD camera by the lens located between the beam-splitter and CCD camera. In the following subsections, we describe the results by carefully observing the spectrum.

4.1 Relative intensity of each order

Fig. 6 shows the spectrum obtained around the strongest orders, which is normalized using the two strongest orders and a blaze function given by Shroeder's book[15]

$$I(\Delta\theta) = \gamma \frac{\sin^2\left[\frac{\pi d \cos\theta}{\lambda}\left\{\sin(\beta - \theta_{\rm B}) + \sin(\alpha - \theta_{\rm B})\right\}\right]}{\left[\frac{\pi d \cos\theta}{\lambda}\left\{\sin(\beta - \theta_{\rm B}) + \sin(\alpha - \theta_{\rm B})\right\}\right]^2}, \quad (2)$$

*The mosaic grating provides an additional advantage for an echelle spectrograph with a γ angle. Since the distortion of the diffracted beam shape is smaller than that of a single grating, it has advantage that the size of the back-end optics can be reduce and the aberration is relatively easier to be corrected.

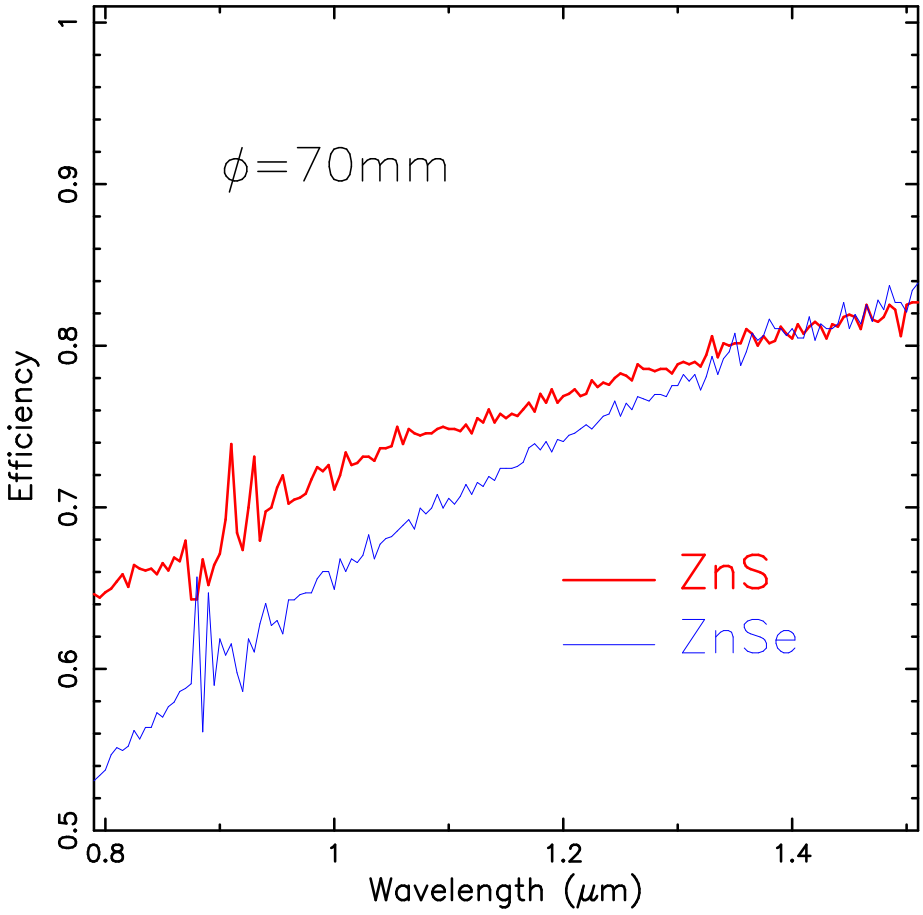

Figure 3. Transmittance of both ZnSe and ZnS immersion gratings with the collimator beam diameter of 70 mm, which calculated with internal attenuation presented by Ikeda et al.[9]

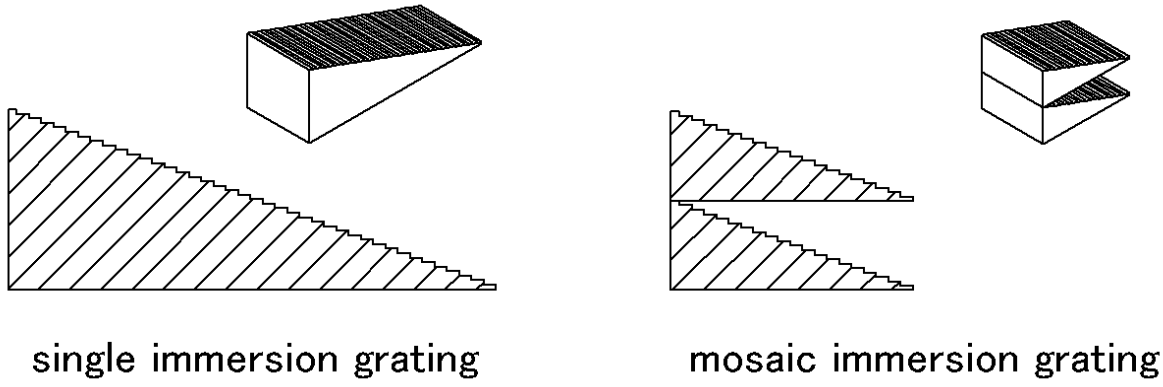

Figure 4. Schematics of single immersion grating (left) and mosaic immersion grating (right). Both gratings have the same clear aperture, but the mosaic one has the shorter optical path than the single one resulting in improvement of the throughput (see text for more details).

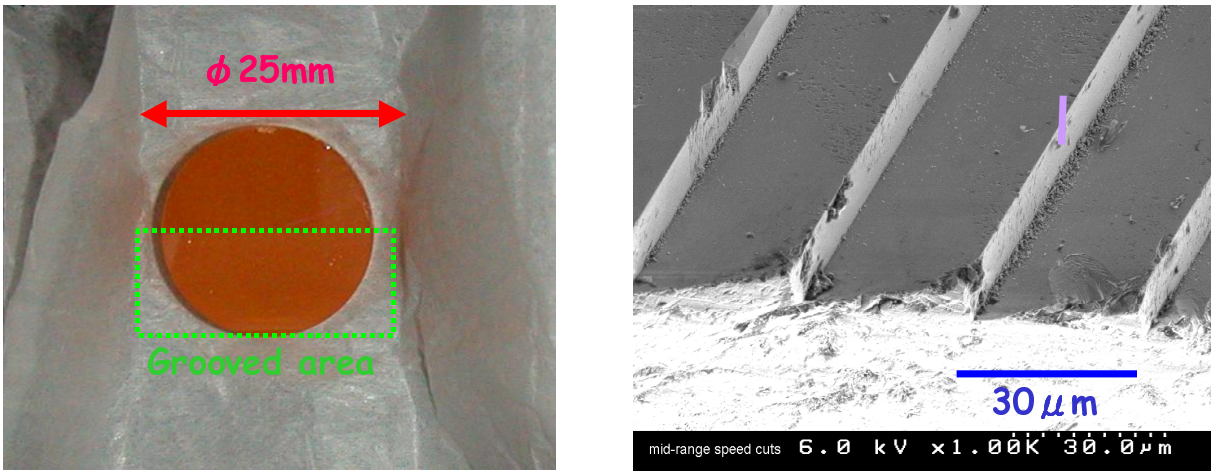

Figure 5. Pictures of test grating (left) and grooves by SEM (right). The grooves are produced in the lower half of the disk substrate.

where α and β are the incidence and diffraction angles, $\Delta\theta$ is the diffraction angle measured from the optical axis corresponding to $\beta - \theta_{\rm B}$, γ is the vignetting factor due to the shadowing effect[16] presented by

$$\gamma = \begin{cases} 1, & \text{for } \alpha \geq \beta \\ \frac{\cos\beta}{\cos\alpha}, & \text{for } \alpha < \beta. \end{cases} \tag{3}$$

From Fig. 6, the side-lobe orders (m = 84 and 87) well agree with or falls bellow the blaze function curve, which indicates that the diffraction light strongly concentrates on the main order, thereby suggesting the high diffraction efficiency. This is consistent with the sharp groove corner with the radius of < 0.2 μm shown in Fig. 5.

4.2 Background scattered light

The measured background scattered light seen between the main orders is integrated to be $I_{\rm bk}/\sum I \simeq 1.3$ % where $\sum I$ is the total intensity of the diffracted light. In principle, the scattered light is primarily produced by the surface roughness and the random groove pitch error. Each intensity is given by

$$\frac{I_{\rm r}}{\sum I} = \left(\frac{4\pi n \sigma_H}{\lambda}\right)^2, \tag{4}$$

and

$$\frac{I_{\rm p}}{\sum I} = \left(\frac{4\pi n \sigma_d \sin\theta}{\lambda}\right)^2, \tag{5}$$

for the surface roughness σ_H and for the pitch error σ_d, respectively. We measured the surface roughness to be 4.8 nm (rms) (see Section 3), which can produce the scattered light of 0.9 % from Eq.(4). Therefore, a component of a random pitch error in the scattered light is estimated to be ~ 0.4 % (= 1.3% − 0.9%). From Eq.(5), the equivalent random pitch errors is 3.5 nm (rms).

When used as an immersion grating, the integrated background scattered light should is 3.1% at $\lambda = 1$ μm because it is magnified by $(n/\lambda)^2$ from Eq.(4) and (5). The energy loss is negligible compared to that by the bulk scattering of CVD-ZnSe, and is acceptable for a general purpose spectrometer for astronomy.

4.3 Ghost

Any obvious Rowland or Lyman ghosts are not visible in our spectrum. However, since the ghosts could be submerged in the diffraction ripple pattern, which prominently appears if the number of grooves across the

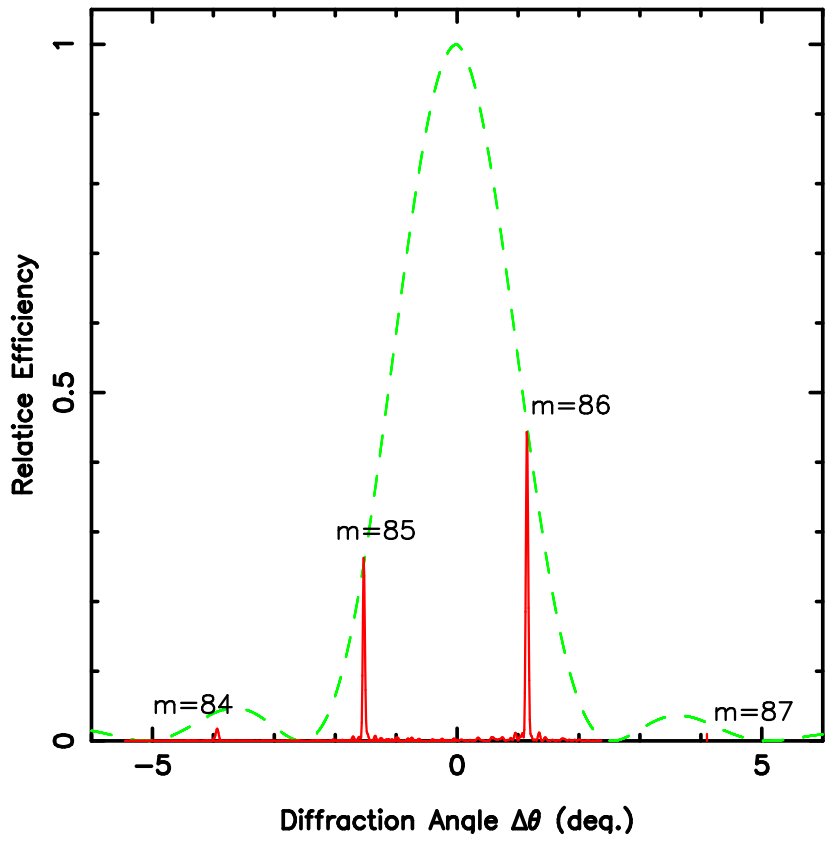

Figure 6. Obtained spectra at 633 nm around the main order. The dashed line presents the blaze function defined as Eq.(2).

incident beam, N, is extremely small[17] ($N = \phi/(d\cos\theta_{\rm B}) \sim 40$ in our case), the ghost light less than the level of 10^{-2} of the main order is very difficult to be identified from the forest of the diffraction pattern (see Fig. 7). Instead, we estimate the upper limit of total intensity of ghosts by comparing the measured total intensity of sub-peaks between orders (13.4%) and the predicted intensity of the diffraction pattern by the scalar diffraction theory (9.7%). The resultant total intensity of Rowland/Lyman ghosts is less than 3.7% (=13.4% − 9.7%).

4.4 Estimation of diffraction efficiency

The maximum relative diffraction efficiency is estimated to be $\geq 87.4\%$ at $\lambda = 0.633$ nm, which is obtained by assuming the energy loss due to the scattered light (1.3%) and ghost ($\leq 3.7\%$) from the maximum diffraction efficiency at $m = 86$, $I_{86}/\sum I_k$, where I_k is the intensity of k-th order, predicted by Eq.(2). When used as an immersion grating at $\lambda = 1$ μm, the relative diffraction efficiency is estimated to be $\geq 81\%$ since the scattered light is magnified by $(n/\lambda)^2$ from Eqs.(4) and (5). The absolute diffraction efficiency can be also estimated to $\geq 65\%$ at 1μm if including (i) the internal attenuation discussed in Section 2 ($\leq 13\%$), (ii) the imperfection of BBAR (Broad-Band Anti-Reflection) coating on the entrance/exit surface of the immersion grating ($\leq 2\%$), and (iii) the absorption of metal coating on the diffraction surface ($\leq 5\%$), as the additional energy loss.

5. SUMMARY AND FUTURE WORK

We are developing a ZnSe immersion grating for a high resolution spectrograph in the short NIR region, WINERED. We eliminated the internal attenuation of ZnSe and ZnS (the latter is also a candidate for the immersion grating) and concluded that they are usable, in particularly, if adopting a mosaic type immersion

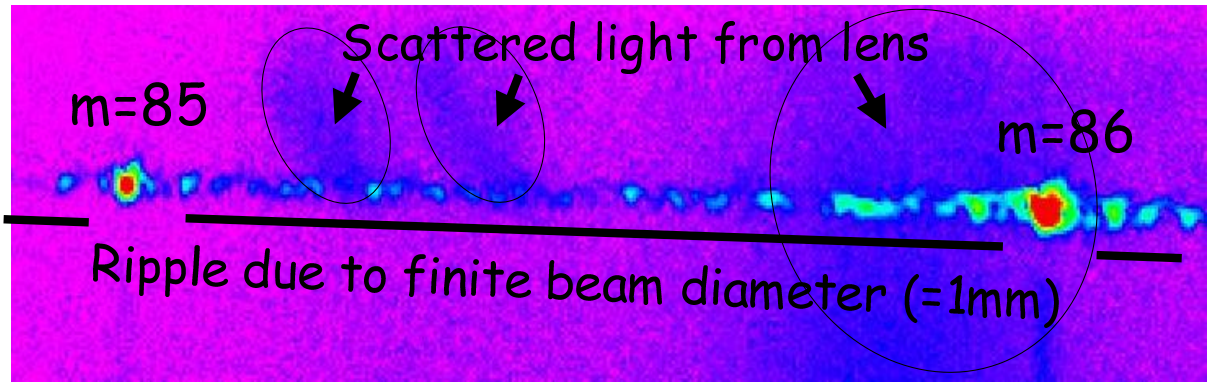

Figure 7. Two-dimensional spectrum obtained by the optical testing with HeNe laser. For the purpose of visualization, the level of the intensity is presented in the logarithmic scale. We can clearly see the diffraction patterns between two orders of $m = 85$ and 86. These patterns are not ghosts but are almost attributed to the diffraction patterns due to the small size of beam (see text for more details).

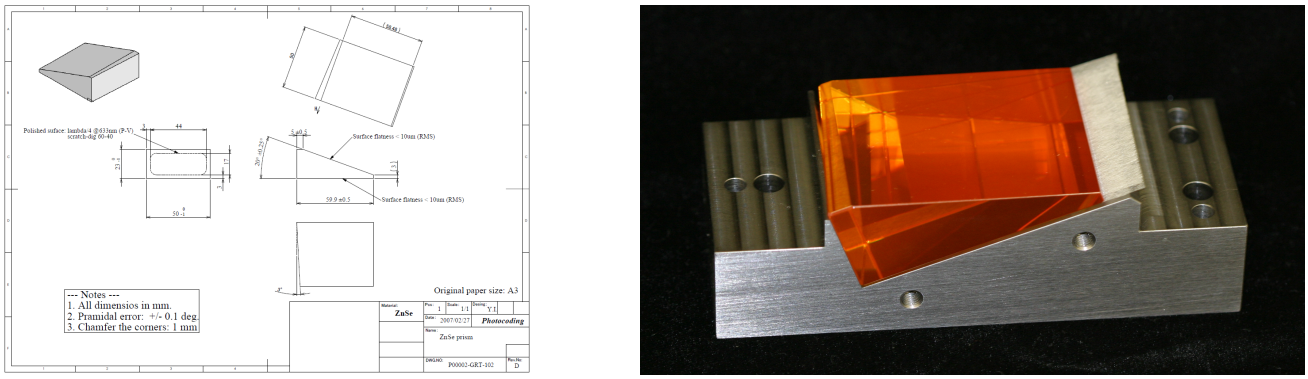

Figure 8. Drawing of a large ZnSe prism for the first completed immersion grating (left) and picture of the polished ZnSe prism grating mounted on the fixture (right).

grating. Then, we fabricated a ZnSe sample grating with the same groove pitch and blaze angle to those required by WINERED, using the nano precision fly-cutting machine, PERL II, at LLNL. This grating shows the low scattered light and little ghost, and the high relative diffraction efficiency $> 80\%$, which satisfies our specification of a device for astronomical NIR spectroscopy.

As a next step, we plan to try to fabricate a large ZnSe immersion grating (with an entrance aperture of 23mm $\times$ 50mm and a blaze angle of 70°) by directly cutting the grooves on the polished surface of a ZnSe prism as shown in Fig. 8 (left). We have prepared for a ZnSe prism and a fixture for stably holding the prism on PERL II (see the right of Fig. 8). The machining process will be finished by the end of this summer. We will evaluate the optical performance of this immersion grating with similar methods described in Section 4 using visible and IR laser by the end of 2008.

ACKNOWLEDGMENTS

We would like to thank A. Tokunaga for fruitful suggestions and comments through this project. A portion of optical measurements were carried out using equipments in Advanced Technology Center (= ATC) of National Astronomical Observatory in Japan. We feel most grateful to the staffs of ATC, especially to K. Mitsui. The

fabrication of the sample grating was performed under the auspices of the U. S. Department of Energy by Lawrence Livermore National Laboratory under Contract DE-AC52-07NA27344. This study was supported by KAKENHI(16684001) Grant-in-Aid for Young Scientists (A) and KAKENHI(20340042) Grant-in-Aid for Scientific Research (B) by Japan Society for the Promotion of Science. It is also supported by the Grant for the Space Instrument Basic Development (FY2007) by ISAS. S.K. and C.Y. were financially supported by the Japan Society for the Promotion of Science (JSPS).

REFERENCES

[1] Yasui, C., Ikeda, Y., Kondo, S., Motohara, K., Minami, A., and Kobayashi, N., "Warm infrared Echelle spectrograph (WINERED): testing of optical components and performance evaluation of the optical system," in [*Ground-based and Airborne Instrumentation for Astronomy II. Proceedings of the SPIE, 7014-108*], *Presented at the Society of Photo-Optical Instrumentation Engineers (SPIE) Conference* **7014** (June 2008).

[2] Yasui, C., Ikeda, Y., Kondo, S., Motohara, K., and Kobayashi, N., "WINERED: optical design of warm infrared echelle spectrograph," in [*Ground-based and Airborne Instrumentation for Astronomy. Edited by McLean, Ian S.; Iye, Masanori. Proceedings of the SPIE, Volume 6269, pp. 62694P (2006).*], *Presented at the Society of Photo-Optical Instrumentation Engineers (SPIE) Conference* **6269**, 62694P (July 2006).

[3] Sebring, T. A., Moretto, G., Bash, F. N., Ray, F. B., and Ramsey, L. W., "The Extremely Large Telescope (ELT), a scientific opportunity; an engineering certainty," in [*Proceedings of the Backaskog workshop on extremely large telescopes*], Andersen, T., Ardeberg, A., and Gilmozzi, R., eds., 53 (2000).

[4] Monnet, G. and Gilmozzi, R., "Status of the ESO ELT," in [*The Scientific Requirements for Extremely Large Telescopes*], Whitelock, P., Dennefeld, M., and Leibundgut, B., eds., *IAU Symposium* **232**, 429–431 (2006).

[5] Gilmozzi, R. and Spyromilio, J., "The European Extremely Large Telescope (E-ELT)," *The Messenger* **127**, 11–+ (Mar. 2007).

[6] Ikeda, Y., Kobayashi, N., Kondo, S., Yasui, C., Motohara, K., and Minami, A., "WINERED: a warm near-infrared high-resolution spectrograph," in [*Ground-based and Airborne Instrumentation for Astronomy. Edited by McLean, Ian S.; Iye, Masanori. Proceedings of the SPIE, Volume 6269, pp. 62693T (2006).*], *Presented at the Society of Photo-Optical Instrumentation Engineers (SPIE) Conference* **6269**, 62693T (July 2006).

[7] Kaeufl, H.-U., Ballester, P., Biereichel, P., Delabre, B., Donaldson, R., Dorn, R., Fedrigo, E., Finger, G., Fischer, G., Franza, F., Gojak, D., Huster, G., Jung, Y., Lizon, J.-L., Mehrgan, L., Meyer, M., Moorwood, A., Pirard, J.-F., Paufique, J., Pozna, E., Siebenmorgen, R., Silber, A., Stegmeier, J., and Wegerer, S., "CRIRES: a high-resolution infrared spectrograph for ESO's VLT," in [*Ground-based Instrumentation for Astronomy*], Moorwood, A. F. M. and Iye, M., eds., *Presented at the Society of Photo-Optical Instrumentation Engineers (SPIE) Conference* **5492**, 1218–1227 (Sept. 2004).

[8] Marsh, J. P., Mar, D. J., and Jaffe, D. T., "Production and evaluation of silicon immersion gratings for infrared astronomy," *Applied Optics* **46**, 3400–3416 (June 2007).

[9] Ikeda, Y., Kobayashi, N., Kondo, S., Yasui, C., Tokoro, H., and Terada, H. in preparation (2008).

[10] Kuzmenko, P. J., Davis, P. J., Little, S. L., and Hale, L. C., "Materials and fabrication issues for large machined germanium immersion gratings," in [*Optomechanical Technologies for Astronomy. Edited by Atad-Ettedgui, Eli; Antebi, Joseph; Lemke, Dietrich. Proceedings of the SPIE, Volume 6273, pp. 62732W (2006).*], *Presented at the Society of Photo-Optical Instrumentation Engineers (SPIE) Conference* **6273**, 62732W (July 2006).

[11] Kuzmenko, P. J., Davis, P. J., Little, S. L., Little, L. M., and Bixler, J. V., "High efficiency germanium immersion gratings," in [*Optomechanical Technologies for Astronomy. Edited by Atad-Ettedgui, Eli; Antebi, Joseph; Lemke, Dietrich. Proceedings of the SPIE, Volume 6273, pp. 62733T (2006).*], *Presented at the Society of Photo-Optical Instrumentation Engineers (SPIE) Conference* **6273**, 62733T (July 2006).

[12] Kuzmenko, P. J., "Prospects for machined immersion gratings in the near infrared and visible," in [*Optomechanical Technologies for Astronomy. Edited by Atad-Ettedgui, Eli; Antebi, Joseph; Lemke, Dietrich. Proceedings of the SPIE, Volume 6273, pp. 62733S (2006).*], *Presented at the Society of Photo-Optical Instrumentation Engineers (SPIE) Conference* **6273**, 62733S (July 2006).

[13] Kuzmenko, J. P., Little, S. L., Ikeda, Y., and Kobayashi, N., "Fabrication and testing of diamond-machined gratings in ZnSe, GaP, and bismuth germanate for the near infrared and visible," in [*Advanced Optical and Mechanical Technologies in Telescopes and Instrumentation. Proceedings of the SPIE, 7018-181*], *Presented at the Society of Photo-Optical Instrumentation Engineers (SPIE) Conference* **7018** (June 2008).

[14] Ikeda, Y., Kobayashi, N., Terada, H., Shibayama, A., Ozawa, A., Yasui, C., Kondo, S., Pyo, T., and Kawakita, H., "High-efficiency silicon immersion grating by electron-beam lithography for high-resolution NIR spectroscopy," in [*Ground-based and Airborne Instrumentation for Astronomy II. Proceedings of the SPIE, 7014-226*], *Presented at the Society of Photo-Optical Instrumentation Engineers (SPIE) Conference* **7014** (June 2008).

[15] Schroeder, D. J., [*Astronomical Optics; 2nd edition*], Academic Press, San Diego (2000).

[16] Bottema, M., "Echelle efficiencies: Theory and experiment - Comment," *Applied Optics* **20**, 528–530 (Feb. 1981).

[17] Kubota, H., [*Applied Optics*], Iwanami, Tokyo (1959).